Journal of Cellular Biochemistry 61:81–96 (1996)

Intracellular Localization of the mRNAs of Argininosuccinate Synthetase and Argininosuccinate Lyase Around Liver Mitochondria, Visualized by High-Resolution In Situ Reverse Transcription-Polymerase Chain Reaction

Natalie S. Cohen

Department of Molecular Pharmacology and Toxicology, University of Southern California School of Pharmacy, Los Angeles, California 90033

Abstract Argininosuccinate synthetase and argininosuccinate lyase, two cytoplasmic enzymes of the urea cycle, are released into the soluble phase in the absence of detergent when cells are disrupted. Yet previous biochemical studies, as well as immunocytochemistry at the electron microscope level, have shown that these enzymes are localized around mitochondria in situ. Such intracellular localization of soluble enzymes requires mechanisms to deliver the proteins to the appropriate sites, where they may then be anchored by specific protein–protein interactions. A method was developed to examine the intracellular distribution of the mRNA of argininosuccinate synthetase and argininosuccinate lyase in intact rat liver at the ultrastructural level by in situ reverse transcription and the polymerase chain reaction, using primers targeting regions of the coding sequences of the rat enzymes, digoxigenin-dUTP as the label, and anti-digoxigenin/10 nm gold plus silver enhancement as the detection method. The tissue was fixed in 4% paraformaldehyde/0.1% glutaraldehyde and embedded in Lowicryl. Examination of the numbers and the location of the silver grains, coupled with morphometric analysis of the electron micrographs, permitted the calculation of the silver "enrichment ratio" for each type of cell structure. These ratios showed that the mRNAs for argininosuccinate synthetase and argininosuccinate lyase were located next to the cytoplasmic side of the mitochondrial membrane and in the nearby endoplasmic reticulum. Most of the silver grains that were observed in the endoplasmic reticulum were within 200 nm of the mitochondria; it was not possible, however, to determine if those grains were actually associated with the reticular membranes. These studies demonstrate that the mRNAs of these two soluble cytoplasmic proteins are localized to the same limited regions where the proteins are situated. Translation of the proteins, therefore, must occur at these specific sites. The targeting of argininosuccinate synthetase and argininosuccinate lyase mRNAs to the immediate vicinity of the mitochondria may be the first step of the mechanisms by which the spatial organization of these soluble proteins in situ is accomplished. The targeting of mRNAs for soluble cytoplasmic proteins of organized metabolic pathways has not been demonstrated previously. These studies also show that in situ reverse transcription and the polymerase chain reaction at the ultrastructural level, which has not been previously reported, can be used to detect specific mRNAs; it should be extremely valuable for the intracellular detection of low-abundance mRNAs.

Key words: mRNA sorting, mRNA targeting, urea cycle, enzyme organization, cell organization, electron microscopy, digoxigenin

Abbreviations used: RT, reverse transcription; PCR, polymerase chain reaction; ASS, argininosuccinate synthetase; ASL, argininosuccinate lyase; ER, endoplasmic reticulum.

Received August 3, 1995; accepted September 28, 1995.

Address reprint requests to Natalie S. Cohen, Department of Molecular Pharmacology and Toxicology, PSC 619, University of Southern California School of Pharmacy, 1985 Zonal Avenue, Los Angeles, CA 90033.

The sorting of specific mRNAs to particular intracellular locations has been demonstrated in somatic cells for proteins of the cytoskeleton [Sundell and Singer, 1990] and of developing myofibrils [Isaacs and Fulton, 1987] and neuronal processes [Kleiman et al., 1994]. Directed mRNA transport is an important aspect of mRNA metabolism and gene regulation, of obvi-

ous importance for the proper assembly of those well-described, morphologically distinct structural elements of the cell.

While the cytoskeleton and many other structures can be visualized by microscopy, there is another level of organization within the cell that can be demonstrated only by biochemical techniques. This is the level of the intracellular organization of soluble enzymes. Some complex metabolic pathways are catalyzed by enzymes that may show little affinity for each other when in dilute solution, but which function in situ as spatially ordered systems [Srere, 1987]. This is an extremely important and basic feature of cells. The characteristics of such pathways within the cell suggest that the specific organization of the individual enzymes is necessary for proper function. No information is available about the mechanisms underlying the localization of these separate enzyme proteins.

A good example of such an enzyme system which is organized only in situ is the urea cycle of mammalian liver. This pathway consists of five reactions, of which the first two occur exclusively in the mitochondrial matrix [Gamble and Lehninger, 1973; Clarke, 1976], and the next three in the cytoplasmic compartment [Ratner, 1976]. All the urea cycle enzymes are soluble; i.e., they go into solution readily in the absence of detergent when mitochondria or cells are disrupted. The behavior of the individual enzymes in solution, however, does not account for several characteristics of the operation of the pathway in situ [Cohen et al., 1980, 1982, 1985, 1987, 1992; Cheung et al., 1989]. In previous biochemical work using intact and permeabilized isolated liver mitochondria and hepatocytes, we reported that intermediates are channeled at each step of the pathway, showing that the enzymes are sequentially organized [Cohen et al., 1987, 1992; Cheung et al., 1989]. Since channeling occurs even across the mitochondrial membranes, these data also showed that the three cytoplasmic members of the pathway are located next to the mitochondria [Cheung et al., 1989]. In recent immunocytochemical studies of intact liver at the electron microscope level [Cohen and Kuda, 1996], we confirmed this location for argininosuccinate synthetase (ASS) and argininosuccinate lyase (ASL); nearly all the ASS and ASL are organized around mitochondria.

The localization of soluble cytoplasmic enzymes to specific regions of the cell requires mechanisms to direct newly synthesized proteins to the appropriate intracellular sites, or, alternatively, to target specific mRNAs to those sites for translation. The phenomenon of mRNA targeting is firmly established for the cell structures described above; it is possible that the localization of some soluble cytoplasmic enzymes to particular intracellular sites also involves this mechanism.

A method was developed to study the intracellular distribution of ASS and ASL mRNAs in rat liver at the ultrastructural level, using in situ RT-PCR (reverse transcription and the polymerase chain reaction). The results indicate that these mRNAs are localized to areas of the cytoplasm adjacent to, or in the immediate vicinity of, the mitochondria. This may represent the first step in the mechanisms whereby the in situ organization of the cytoplasmic enzymes of the urea cycle is achieved. Targeting of the mRNAs for soluble cytoplasmic enzymes, which has not previously been demonstrated, may be of general importance in the compartmentation of different metabolic pathways to different regions of the cell. In addition to these findings, the present work shows that the new method described, which successfully identifies specific mRNAs at the ultrastructural level, should be valuable for the detection of mRNAs of low abundance.

MATERIALS AND METHODS

Animals and Tissue Preparation

Male Sprague-Dawley rats (160–180 g) were from Simonsen Laboratories (Gilroy, CA). Rats were fed a diet containing 60% protein for 8 days in order to raise the levels of mRNA of the urea cycle enzymes [Morris et al., 1987]. The animals were sacrificed by cervical dislocation, and the liver was removed at once. One mm slices of liver were fixed in 4% paraformaldehyde/0.1% glutaraldehyde in 0.1 M phosphate buffer, pH 7.4, for 1.5 h; 1-mm cubes were then dehydrated in graded alcohols and embedded in Lowicryl (Ted Pella, Redding, CA). Thin sections were picked up on parlodion-filmed nickel grids. Electron microscopy (JEOL 1200CX microscope) was done in the Department of Anatomy and Cell Biology at USC.

Oligonucleotide Primers

The primers (19–22 bases long) targeted regions of the coding sequences of rat ASS [Surh

et al., 1988] or ASL [Amaya et al., 1988], or a sequence of subunit III of rat cytochrome oxidase (COIII) [Gadeleta et al., 1989], which is a mitochondrially coded peptide of the inner mitochondrial membrane. The cDNA sequences used for ASS were 5'GTGGAAGAGTTCATCTGGC3' (sense primer, ASS-1), and 5'CCGTGAGACACATACTTGG3' (antisense primer, ASS-2); these targeted a fragment of 145 nt. For ASL, the sequences were: 5'CACCATGGACAAGTTCAACTC3' (sense primer, ASL-3), and 5'CTTGTCCAGGCCTTGCAGTATC3' (antisense primer, ASL-4); these bracket a fragment of 150 nt. For COIII, the sequences used were 5'CTAACAGGAGCCCTATCAGCT3' (sense primer, COIII-1), and 5'AGGATTATTCCGTATCGGAGG3' (antisense primer, COIII-2). These sequences represent nt 8635–8655, and 8817–8837, respectively, of the rat COIII sequence described by Gadeleta et al. [1989], and define a 203-nt fragment. The primers were synthesized by the Microchemical Core Laboratory of the Norris Comprehensive Cancer Center at the University of Southern California School of Medicine.

Before use in the in situ experiments, each of the primer pairs was tested in in vitro PCR reactions, and $MgCl_2$ was titrated, using total rat liver cDNA preparations as the template. Total rat liver RNA was isolated by the rapid guanidinium isothiocyanate method [Chomczynski and Sacchi, 1987]; the preparation had a 260/280 nm absorbance ratio of 1.8. Reverse transcription of aliquots of the total RNA preparation was performed at once, by the method described by Horikoshi et al. [1992]. The PCR mixture used was as described by Horikoshi et al. [1992], with $MgCl_2$ concentrations from 1.0 to 4.0 mM. The reaction mixtures were heated to 95°C for 3 min, subjected to 30 cycles of 95°C and 55°C (1 min each), and then held at 72°C for 15 min, using a Perkin-Elmer Thermal Cycler 480. The PCR products were electrophoresed on 7% acrylamide/7 M urea gels and the gels examined under UV illumination; each of the primer pairs produced a single PCR product band of the appropriate size. The optimal $[Mg^{2+}]$ was 2.5 mM for the ASS primers, and 2.0 mM for the ASL and COIII primers; the appropriate $[MgCl_2]$ for each primer pair was used for in situ PCR.

Treatment of Thin Sections

All reagents used were of molecular biology grade, and all solutions were prepared with diethyl pyrocarbonate-treated water. The method used for in situ RT-PCR was based on those currently used for paraffin sections [Nuovo et al., 1993]. Of a variety of conditions used for various steps of the procedures, those described below gave the best results. The backs of the electron microscope grids were marked at one edge with a small dot of indelible ink so that the side with the sections could be easily recognized during the experimental procedures.

The grids were floated section side down, in porcelain spot plates, on 40-μl droplets of Proteinase K (1 mg/ml in 30 mM Tris–HCl, pH 8.0, 50 mM KCl, 6 mM $MgCl_2$, 20 mM EDTA) for 15 min at 37°C; the wells were tightly covered with Parafilm during the incubation. The reactions were stopped by the addition of 0.4 ml of water, and the grids were transferred to 0.5-ml microcentrifuge tubes and washed 6 times (3 min each) with TE buffer (10 mM Tris, 1 mM EDTA, pH 8.0). The tubes were heated to 95°C for 3 min to denature the protease. The grids were then exposed to 100 μl of a DNase solution (1 U/μl in 0.1 M sodium acetate, 5 mM $MgCl_2$, pH 5.0, with 25 μl RNAguard/ml) overnight at 37°C, in caps removed from 1.7-ml microcentrifuge tubes; the caps were covered with Parafilm. The grids were then washed and heated as above. The RT reaction mixture used was as described by Horikoshi et al. [1992], except that 1 μM of the antisense oligonucleotide was used as a primer instead of random hexamers; *incubations* were on 40 μl in microcentrifuge tube caps (covered), for 10 min at room temperature, and then 40 min at 42°C. The grids were drained, put into 0.5-ml PCR tubes containing 20 μl of PCR mixtures [Horikoshi et al., 1992], containing 1 μM concentration of each primer, and 10.5 μM digoxigenin-11-dUTP (the ratio of dTTP to digoxigenin-dUTP was 19:1). $MgCl_2$ concentrations were 2.5 mM for reactions with the ASS primers and 2.0 mM for ASL and COIII primers. A PCR-Gem was added to each tube, the tubes were heated to melt the wax, cooled, and 5 μl (0.65 units) of AmpliTaq DNA polymerase was added. The tubes were heated to 95°C for 3 min, cycled at 95°C and 65°C, 1 min each, for 7 cycles, held at 72°C for 15 min, and cooled. The tubes were cut to recover the grids, which were washed thoroughly in 0.15 M NaCl, 15 mM sodium citrate.

In each experiment the treatment of some grids was terminated after the RT reaction; i.e., there was no PCR. In such cases the digoxigenin-dUTP was included in the RT step, and the grids

were then washed and the digoxigenin-dUTP detected as described below. Control reactions consisted of using the sense primer or omitting the primer in the RT step and of omitting the digoxigenin.

In the process of developing the method, a number of conditions were tested, all of which produced the same general findings, although the best results were obtained with the method described in detail above. For example, in some experiments, the ratio of dTTP to digoxigenin-dUTP during the PCR was varied between 15 and 20; the number of PCR cycles was 30; and the annealing/extension temperature used in the PCR was 55°C instead of 65°C. Other variations consisted of the omission of either the initial DNase treatment, or RT, or both, before the PCR was performed. In some experiments in which the procedures were terminated after the RT step, the ratio of dTTP to digoxigenin-dUTP during RT was varied between 15 and 25. These variations are noted in the Results section where applicable.

Detection

The grids were washed twice (15 min each) in 0.15 M NaCl, 15 mM sodium citrate at 50°C in spot plates, and twice (5 min each) in phosphate-buffered saline, pH 7.4, at room temperature. The grids were blocked for 15 min, exposed for 1 h to anti-digoxigenin coupled to 1 nm gold, and then silver enhanced for 11–12 min, all as described in [Fischer et al., 1992]. The final washing, blocking, and detection steps were performed by floating the grids on droplets on pieces of Parafilm. The droplets and grids were covered with an inverted petri dish during these steps to retard evaporation, and also with an opaque box during the anti-digoxigenin and silver enhancement steps. The grids were thoroughly washed (6 washes, 5 min each) on large drops of HPLC-grade water after silver enhancement.

Analysis of Recovered Reaction Mixtures

In every experiment, the RT reaction mixtures and the PCR mixtures were recovered, and electrophoresed on 7% acrylamide/7% urea gels in order to determine whether reaction products had escaped from the thin sections. In addition, in each PCR experiment, parallel tubes containing a reagent blank and a soluble cDNA standard for each primer pair used were included so that it could be ascertained that the PCR had proceeded as expected; these samples were also electrophoresed. The gels were examined under UV illumination, and then were transferred to nylon membranes (Boehringer Mannheim) in 0.89 M Tris-borate, pH 8.3, 25 mM EDTA in an ABN semidry transfer apparatus. The membranes were treated according to the Genius protocol (Boehringer Mannheim) for the detection of digoxigenin, and exposed to Kodak XRP film.

Quantitative Morphometry

The relative amounts of mitochondrial matrix, mitochondrial outer membrane, endoplasmic reticulum (ER), nuclei, and "other" structures were determined by the point counting method [Weibel and Bolender, 1973], and the total numbers of silver grains and their location were scored. Point counting was done by overlaying the micrographs with a regular grid of intersecting lines, and counting the number of intersections that fell over each of the recognizable structures of interest; the "density" of each structure in a micrograph is the percentage of the total intersections which fell over that structure. The "relative frequency" of silver over each structure is equal to the number of grains over that structure as a percentage of the total silver grains on the micrograph. From these data the ratios of "relative frequency" to "density" were calculated for each type of structure. Random background silver grains generate a ratio of relative frequency to density of 1.0 or lower. Ratios greater than 1.0 indicate that there is a preferential association of the signal with the structure in question [Weibel and Bolender, 1973].

In addition to the above analysis, the location of each of the silver grains in the ER was scored according to its distance (in 100-nm increments) from the nearest mitochondrion. All silver grains were also categorized as small, medium, or large. Because there is always some background silver deposited in these procedures, some of the smaller grains may be noise, while it is more likely that medium and large silver grains represent bona fide signal (see Results).

The appearance of the tissue in the thin sections treated according to the experimental procedures described above was not as good as that of untreated thin sections that were merely stained in uranyl acetate, and occasional bits of debris were observed. Despite the fact that there was less ultrastructural detail revealed in the

treated sections, the ER membranes could be resolved, and the mitochondrial cristae were visible. For point counting, the category called "mitochondrial outer membrane" refers to the mitochondrial periphery. For scoring the location of the silver grains in experiments using the ASL or ASS primers, those grains at the mitochondrial periphery which were not clearly on the matrix side were classified as being located at the mitochondrial membrane. For experiments with the COIII primers, silver grains directly over, or on the matrix side of the mitochondrial periphery were classified as mitochondrial membrane-associated. The assessment of the location of the silver grains at the mitochondrial periphery was done with the aid of a magnifying lens, and every effort was made to avoid bias.

Materials

For treatment of the thin sections, DNase I (RNase-free), digoxigenin-11-dUTP, anti-digoxigenin-1 nm gold, bovine serum albumin (molecular biology grade), and silver enhancement reagents were from Boehringer Mannheim (Indianapolis, IN). AmpliTaq DNA polymerase and PCR-Gems were from Perkin-Elmer Cetus (Norwalk, CT), RNAguard RNase inhibitor, deoxyribonucleotide triphosphates, random hexamers, and bovine serum albumin used for RT were from Pharmacia (Alameda, CA), M-MLV reverse transcriptase was from Bethesda Research Laboratories (Gaithersburg, MD). Other molecular biology-grade chemicals, buffers, and enzymes were obtained from Boehringer Mannheim, Fisher Scientific (Tustin, CA), or from Sigma Chemical Co. (St. Louis, MO).

RESULTS

Localization of ASL and ASS mRNAs

Electron micrographs of thin sections subjected to in situ RT-PCR, or to in situ RT without subsequent PCR, are shown in Figure 1 for ASL and Figure 2 for ASS. Quantitative analysis of the electron micrographs showed that, regardless of the specific procedure used, a disproportionately large number of silver grains were touching the cytoplasmic side of the mitochondrial membrane or in the ER in the immediate vicinity of the mitochondria. This was observed both when total silver grains were considered, or when only medium and large silver grains were scored. The latter distinction was made because of the finding that micrographs of control thin sections, in which the digoxigenin-dUTP or the primer had been omitted during the experimental procedures, or the sense primer had been used for RT (without subsequent PCR), had numerous silver grains, which were almost all very small (see below). Thus, it may be more likely that random background silver grains, representing "noise," would fall into the small size category on the experimental sections as well.

In Table I the mean ratios of "relative frequency" of silver grains to "density" are shown for different cell structures under a variety of experimental conditions. When either the ASL or the ASS primers were used, the ratios obtained for mitochondrial outer membrane and for ER were greater than 1.0 under all circumstances, while the ratios for mitochondrial matrix and for "other" structures were always less than 1.0. For example, as shown in the first line of Table I, for RT-PCR using the ASL primers (Fig. 1A), and considering total silver grains, the mean ratios were 2.43 ± 0.48 ($M \pm SEM$) for mitochondrial outer membrane, and 1.37 ± 0.20 for ER. By contrast, the ratios were 0.61 ± 0.11 and 0.87 ± 0.11 for mitochondrial matrix and other structures, respectively. Comparable values were obtained when only medium and large silver grains were considered (Table 1, line 2).

When the digoxigenin-dUTP was included in the RT step, and PCR was omitted, similar results were obtained. For the most part, this protocol resulted in smaller and fewer silver grains (Figs. 1B, 2B), perhaps because lower quantities of digoxigenin-dUTP were incorporated at the site of each mRNA. Nonetheless, the silver grains were preferentially associated with the outer membrane. For example, using the ASL primer the ratios of (total silver) relative frequency to density were 2.37 ± 0.70 for mitochondrial outer membrane and 1.47 ± 0.34 for ER (Table I, line 3). Similar ratios were found when the calculations included only medium/large grains (Table I, line 4). For all other structures the ratios were < 1.0.

The same labeling pattern was observed regardless of the precise protocol employed. For example, when PCR was performed with the ASL primers without prior RT (Table I, lines 5 and 6; Fig. 1C), the procedure still resulted in differential silver labeling, although there were fewer silver grains under these conditions than when RT-PCR was used. The Ampli-Taq DNA

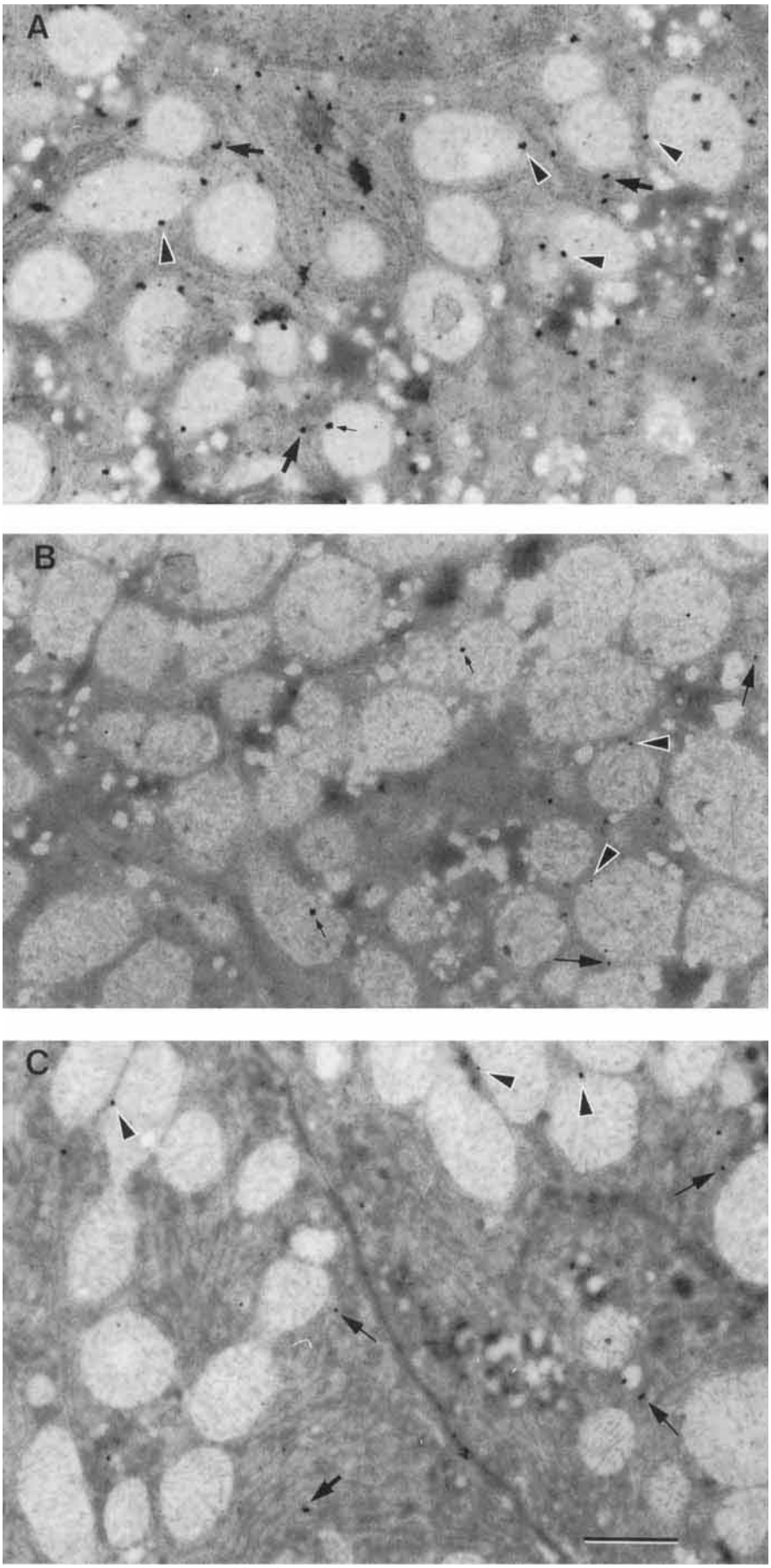

Figure 1.

polymerase used is described by the vendor as having essentially no RT activity, but that characteristic is evaluated under conditions very different from those employed in these studies. There have been several reports of RT activity in Ampli-Taq DNA polymerase [Jones and Foulkes, 1989; Shaffer et al., 1990]. In the present studies, the amount of RT activity in this product, though extremely low, was sufficient to produce some cDNA, which served as a template for the PCR.

The data from all of the micrographs evaluated for ASL mRNA, from experiments using a variety of procedures, were pooled and the ratios obtained are shown in Table I (lines labeled "various"). In the additional experiments included in this group, the ratios of dTTP to digoxigenin were from 16.7:1 to 20:1, the number of PCR cycles was 30, and the annealing/extension temperature was 55°C. These data show that ASL mRNA is preferentially located at the mitochondrial outer membrane and in the ER.

For experiments using the ASS primers, ratios similar to those for ASL were obtained, again regardless of the specific experimental procedures followed. For all silver grains, the ratios for mitochondrial outer membrane were 2.36 ± 0.40 and 2.18 ± 0.33, and those for ER were 1.36 ± 0.20 and 1.19 ± 0.18 after in situ RT-PCR or in situ RT, respectively, while the ratios for mitochondrial matrix and other structures were < 1.0 (Table I, ASS data). Consideration of only medium/large grains gave similar ratios (not shown). Thus, ASS mRNA, like ASL mRNA, is preferentially located at the mitochondrial outer membrane and in the ER.

It is important to note that the ultrastructural details remaining in the treated sections (see below) were not sufficient to reveal if the mRNAs of ASL and ASS which appear to be in the ER close to mitochondria are actually on the rough ER itself, on polyribosomes associated with the mitochondria [Ades and Butow, 1980; Suissa and Schatz, 1982] or on free polyribosomes located near the ER next to the mitochondria.

Localization of COIII mRNA

While ASL and ASS are nuclear-coded cytoplasmic proteins, COIII is coded by the mitochondrial genome, and translated on mitochondrial ribosomes [Attardi and Schatz, 1988]. The COIII peptide is located in the electron transport complex of the mitochondrial inner membrane. COIII mRNA should therefore be found only within mitochondria; labeling COIII mRNA by the procedures described here should result in no preferential association of the silver grains with the ER. When in situ RT-PCR was performed using the COIII primers, the pattern of silver grains was indeed different from that observed with the ASL and ASS primers (Fig. 3 and Table I, COIII data). Ratios greater than 1.0 were obtained for mitochondrial matrix (1.12 ± 0.11) and for mitochondrial membrane (2.56 ± 0.46), whereas the ratios for ER and other structures were < 1.0. Again, similar ratios were obtained when only medium and large grains were scored (not shown). The contrasting pattern of silver labeling obtained using the COIII primers and primers for the cytoplasmic mRNAs of ASL and ASS supports the validity of the methodology used. It is interesting that the ratios obtained with the COIII primers were consistently much higher for the mitochondrial membrane than for the matrix. This suggests that COIII mRNA is actually predominantly associated with those portions of the inner membrane which lie at the mitochondrial perimeter rather than along the cristae.

Controls

In control experiments from which the digoxigenin-dUTP was omitted, only low numbers of extremely small, randomly distributed background silver grains were observed (Table I, control data, line 1). In control experiments in which either the primer was omitted from the RT reaction or the sense primer was used, without subsequent PCR, there were more grains observed, but again, they were extremely small and randomly distributed (Table 1, control data, lines 2 and 3). These results support the validity of making a distinction on the experimental

Fig. 1. In situ RT-PCR, in situ RT, and in situ PCR using ASL primers. **A:** Section treated with DNase, followed by RT, and then PCR with digoxigenin-dUTP as described in the text. **B:** Section treated with DNase, followed by RT with digoxigenin-dUTP as described, except that the dTTP:digoxigenin-dUTP was 15:1; C, section subjected to PCR with digoxigenin-dUTP, using 30 cycles, an annealing/extension temperature of 55°C, and a dTTP:digoxigenin-dUTP of 20:1. *Arrowheads* point to silver grains just outside mitochondria; *large arrows* to grains in the nearby ER; *small arrows* to grains over the mitochondrial matrix. Bar = 1 μm.

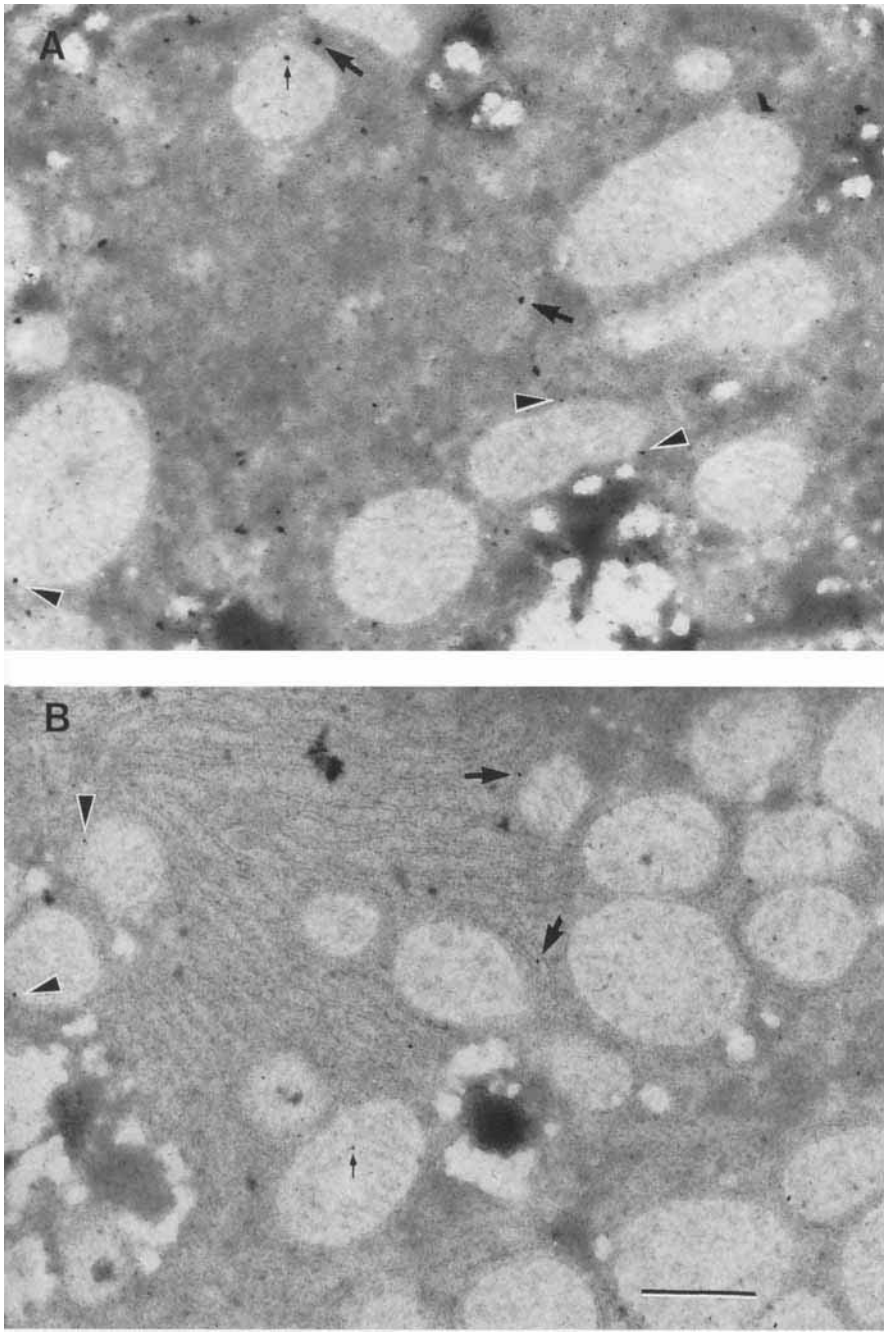

Fig. 2. In situ RT-PCR and in situ RT using ASS primers. **A:** section subjected to PCR with digoxigenin-dUTP, using 30 cycles, an annealing/extension temperature of 55°C, and a dTTP:digoxigenin-dUTP of 16.7:1; **B:** Section treated with DNase, followed by RT with digoxigenin-dUTP, with a dTTP:digoxigenin-dUTP of 15:1. Markings same as for Fig. 1.

sections between total silver grains, some of which are background, and medium to large grains. Since similar ratios were obtained on the experimental sections when total grains or only medium and large grains were considered, however, it appears that only a relatively low number of the small grains on these sections were background.

Quantitative Distribution of ASL and ASS mRNAs Around Mitochondria

The data for ASL and ASS mRNAs in Table I show that the ratios for mitochondrial outer membrane are higher than those for ER, suggesting that these mRNAs are associated most frequently with polyribosomes or ER located imme-

TABLE I. Preferential Association of Silver Grains With Specific Structures After In Situ Treatments of Thin Sections Using Primers for ASL, ASS, and COIII*

		Relative frequency of silver/density of structure					
mRNA	Procedures	Mit. matrix	Mit. outer membrane	ER	Other	No. of EMG	Total grains
ASL	DNase, RT, PCR						
	All silver grains	0.61 ± 0.11	2.43 ± 0.48	1.37 ± 0.20	0.87 ± 0.11	5	576
	Med, Lg grains	0.75 ± 0.15	3.18 ± 0.83	1.40 ± 0.19	0.76 ± 0.12	5	310
	DNase, RT						
	All silver grains	0.64 ± 0.30	2.37 ± 0.70	1.47 ± 0.34	0.64 ± 0.19	4	185
	Med, Lg grains	0.31 ± 0.27	2.75 ± 0.86	1.54 ± 0.37	0.45 ± 0.13	3	85
	DNase, PCR						
	All silver grains	0.79 ± 0.12	1.59 ± 0.60	1.63 ± 0.09	0.70 ± 0.22	3	163
	Med, Lg grains	0.82 ± 0.19	1.56 ± 0.88	1.47 ± 0.14	0.64 ± 0.15	3	122
	Various[a]						
	All silver grains	0.68 ± 0.08	2.18 ± 0.22	1.44 ± 0.08	0.83 ± 0.14	20	1217
	Med, Lg grains	0.66 ± 0.10	2.78 ± 0.35	1.45 ± 0.09	0.55 ± 0.06	18	688
ASS	All PCR[b]						
	All silver grains	0.76 ± 0.09	2.36 ± 0.40	1.36 ± 0.20	0.66 ± 0.11	6	386
	DNase, RT[c]						
	All silver grains	0.77 ± 0.16	2.18 ± 0.33	1.19 ± 0.18	0.73 ± 0.15	5	240
COIII	DNase, RT, PCR						
	All silver grains	1.12 ± 0.11	2.56 ± 0.46	0.88 ± 0.05	0.85 ± 0.03	5	342
Control	No digoxigenin[d]						
	All silver grains	1.25 ± 0.50	0.22 ± 0.27	0.92 ± 0.25	1.08 ± 0.08	3	79
	No primer[e]						
	All silver grains	0.79 ± 0.38	0.84 ± 0.27	0.87 ± 0.15	1.20 ± 0.09	3	131
	Sense primer[f]						
	All silver grains	0.88 ± 0.24	0.84 ± 0.14	0.88 ± 0.11	1.13 ± 0.06	4	219

*Morphometric evaluation of the electron micrographs (EMG) was done as described in the text. The data are grouped according to the experimental procedures used, and the populations of silver grains included in the calculations, i.e., all grains, or only medium plus large (Med, Lg) grains. The values shown are M ±SEM. One EMG represents approximately 206 μm^2 of tissue. Mit, mitochondrial.

[a]Includes all values shown above, plus additional data from experiments using either DNase plus RT-PCR, or RT-PCR without prior DNase, or PCR alone, all with 30 PCR cycles and an annealing/extension temperature of 55°C, with dTTP:digoxigenin dUTP = 16.7:1 to 20:1.

[b]Includes DNase plus RT-PCR; DNase plus PCR; PCR alone; all with 30 PCR cycles and an annealing/extension temperature of 55°C, with dTTP:digoxigenin dUTP = 16.7:1.

[c]dTTP:digoxigenin dUTP = 15:1.

[d]DNase plus RT, using the ASL antisense primer.

[e]DNase plus RT, with dTTP:digoxigenin dUTP = 15:1.

[f]DNase plus RT, using the ASL sense primer, with dTTP:digoxigenin dUTP = 20:1.

diately adjacent to the mitochondrial outer membrane [Shore and Tata, 1975; Ades and Butow, 1980; Suissa and Schatz, 1982]. The ratios for ER, however, were calculated for the entire ER observed on the micrographs, and do not reveal the observed preferential distribution of the silver grains in the ER near the mitochondria. To quantitate that distribution, using the same electron micrographs from which the data in Table I were obtained, the silver grains observed in the ER were plotted against their distance from the mitochondria (Figs. 4, ASL; 5, ASS). These graphs also show the numbers of grains which appeared to touch the outside of the mitochondria. The largest numbers of silver grains were within 100 nm of the mitochondria, predominantly directly in contact with these organelles. One-half to two-thirds as many grains were found at distances of 100–200 nm from the mitochondria, and many fewer grains between 200 and 300 nm. Beyond that distance, the numbers fell off considerably for ASL and leveled off for ASS. This distribution pattern was observed both with the complete RT-PCR protocol (Figs. 4a & 5a) and with the RT procedure alone (Figs. 4b, 5b). Data pooled from various procedures used for the ASL primers are shown in Figure 4c. Similar results were obtained when

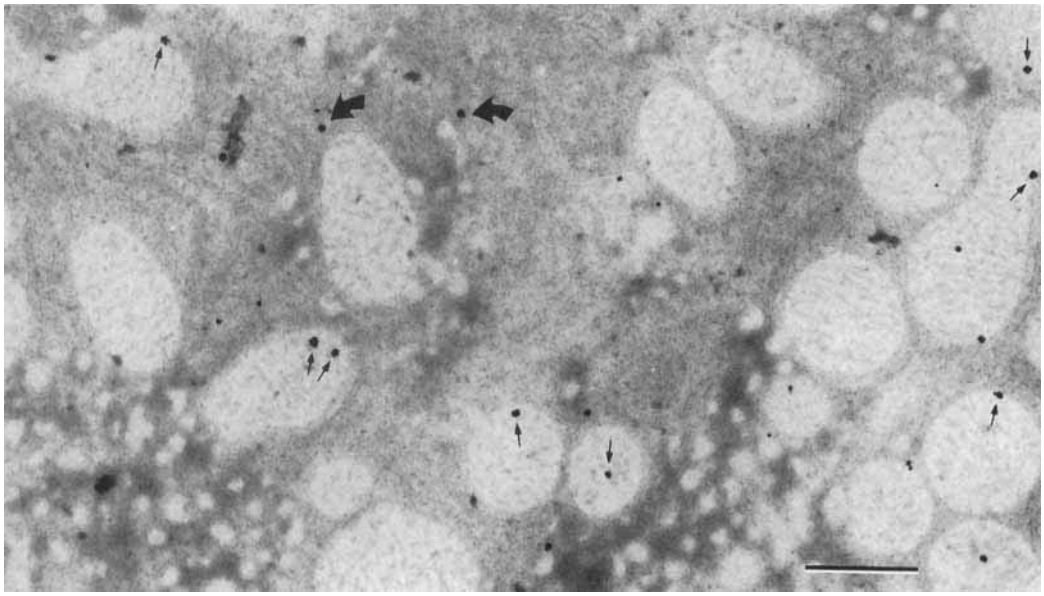

Fig. 3. In situ RT-PCR using COIII primers. Section treated with DNase, followed by RT, and then PCR with digoxigenin-dUTP as described in the text. *Small arrows* point to grains over the mitochondrial periphery or the matrix; *curved arrows* to grains in the ER. Bar = 1 μm.

only medium and large grains were considered; an example is shown for the pooled ASL data (Fig. 4d). Background grains might account for the continued presence of relatively small numbers of grains throughout the ER, although it is also worthwhile to consider that at least some of those silver grains might be in proximity to mitochondria which are just outside the plane of section. The apparently larger numbers of grains at distances beyond 500 nm from the mitochondria reflect the fact that these regions account for a much larger total area of the ER. Taken together with the ratios shown in Table I, these data clearly show that ASL and ASS mRNAs are predominantly located immediately adjacent to the mitochondria or in the ER very near the mitochondrial outer membrane.

By contrast, in experiments using the COIII primers, the distribution of the silver grains in the ER was very different. There were relatively few grains, consistent with the ratio for ER of < 1.0 shown in Table I (COIII data), and there was no gradient of grains in the ER around the mitochondria (Fig. 6, COIII panel). It is likely that the grains in the ER are background. Using the COIII primers, the silver grains were observed to be predominantly over the periphery of the mitochondria or the matrix. Data from control experiments in which either the digoxigenin-dUTP or the primer were omitted from the RT reaction, or the sense primer was used, are also shown in Fig. 6 (Control panel); there were very few grains at the mitochondrial periphery, and silver grains were distributed rather uniformly throughout the ER.

Other Results

Because there were many mitochondria in the thin sections examined, it could be argued that the preferential location of the silver grains representing ASL and ASS mRNAs in the ER very near the mitochondria was an artifact, resulting from there being more ER near the mitochondria than far from them. That this is not the case is shown by the fact that there was a wide range of density of both mitochondria and of ER on the micrographs. Point counting results show that the percentage of total intersecting grid points that fell over the mitochondrial matrix ranged from 12.3 to 21.2, the percentage over mitochondrial outer membrane was from 3.4 to 6.1, over ER from 15.5 to 33.1, and over other structures from 32.1 to 61.8. There was no correlation between the percentage of mitochondrial matrix plus outer membrane and the percentage of ER (correlation coefficient = 0.25 to 0.37).

The appearance of the tissue sections clearly suffered as a result of the experimental procedures used. Electron micrographs of sections that were stained with 3.5% uranyl acetate, but otherwise untreated, show that the tissue was

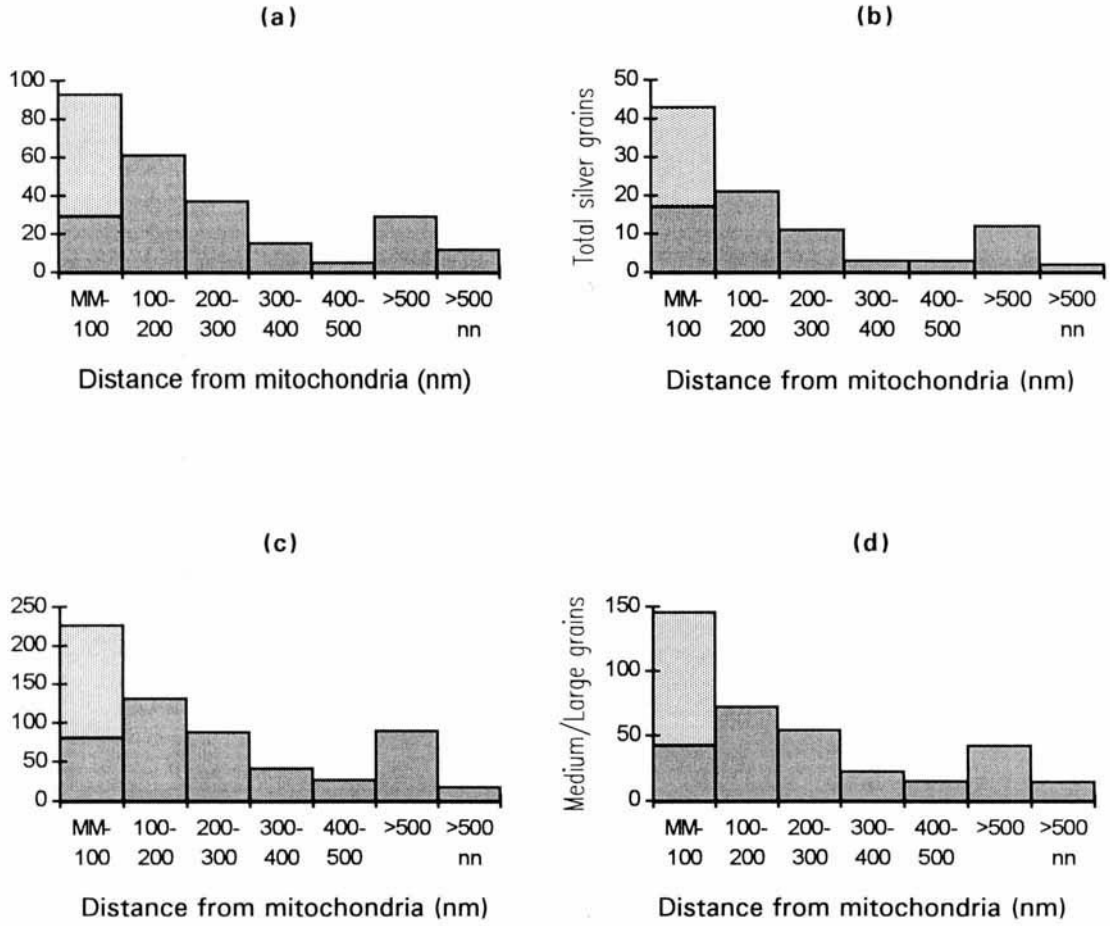

Fig. 4. Distribution of ASL mRNA in the ER around liver mitochondria. The total numbers of silver grains (**a,b,c**) or the numbers of medium and large grains (**d**) observed at the mitochondrial outer membrane or in the ER are plotted versus their distance (nm) from the outer membrane. Bars labeled MM-100 show both the numbers of grains that appeared to be in contact with the membrane (*upper segment of the bars*), and those that did not appear to touch the membrane, but were within 100 nm of it (*lower segment of the bars*). Bar labeled > 500 nn shows the numbers of grains that were more than 500 nm from a visible mitochondrion, but were near the nucleus. The various panels show data obtained after treatment of the thin sections by different procedures, as described in the text: **a:** DNase plus RT-PCR (number of EMG examined = 5). **b:** DNase plus RT (n = 4). **c:** Various procedures, identical to the description in Table I, footnote a (n = 20). **d:** Various procedures as in **c**, but considering only medium and large grains (n = 18).

well fixed and the ultrastructural details well defined (Fig. 7). In treated sections, however, the mitochondria were much less dense than in untreated sections, and much ultrastructural detail was lost. This was most likely caused by the protease treatment. In the untreated section one can see that there are numerous polyribosomes surrounding the mitochondria, and very near the mitochondrial membrane. Some of these polyribosomes, which are not visible in the treated sections, are presumably the sites of ASL and ASS translation. Glycogen was not retained by the fixation and embedding procedures used. Areas where glycogen was lost were seen in all of the sections as "empty" spaces; this would not have affected the experimental procedures used or the results obtained.

The RT and/or PCR products did not escape from the sections in the experiments shown. This was determined by electrophoresing recovered reaction mixtures on 7% polyacrylamide/7 M urea gels and by examining the gels and films of the blotted gels as described in the Methods section. No product bands were detected in these reaction mixtures. This suggests that there was no lateral displacement of products within the sections; since the grids were exposed to relatively large aqueous volumes during the RT and PCR procedures, any dissociation of the products from their site of synthesis would have

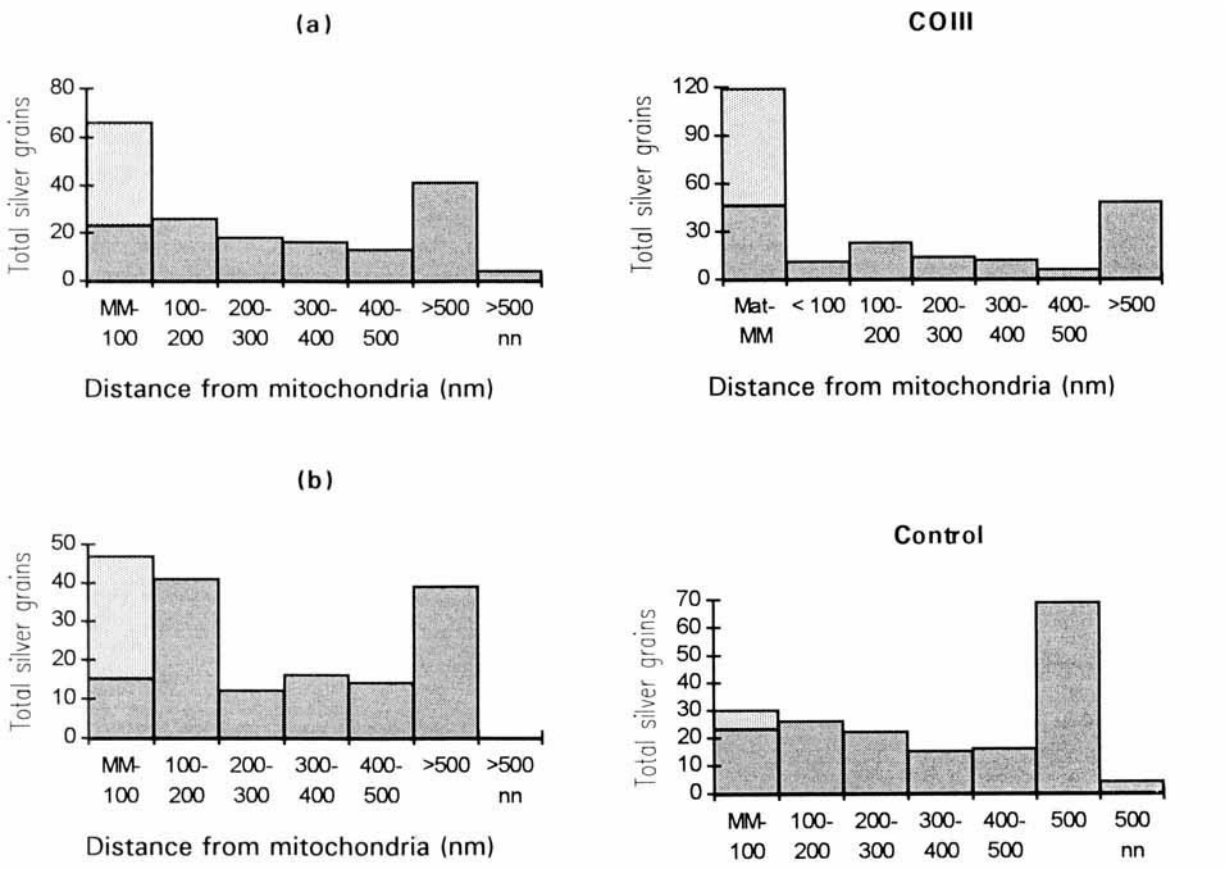

Fig. 5. Distribution of ASS mRNA in the ER around liver mitochondria. The data are plotted as described in the legend for Fig. 4. Total silver grains are shown for thin sections treated as follows. **a:** ± DNase ± RT plus PCR (n = 6). **b:** DNase plus RT (n = 5). The specific conditions used are described in detail in footnotes b and c in Table I.

Fig. 6. Distribution of COIII mRNA in and around liver mitochondria and distribution of grains in the ER in controls. The total numbers of silver grains are plotted versus their location in and around the mitochondria. For the COIII panel, bars labeled Mat-MM show both the numbers of grains observed to be over the mitochondrial matrix (*upper segment of the bars*), plus those over or touching the mitochondrial periphery (*lower segment of the bars*). The other bars show the numbers of grains in the ER at various distances (in nm) from the outer membrane; <100 nm refers to grains that did not appear to touch the membrane but were within 100 nm of it. The data shown are from thin sections treated with DNase plus RT-PCR (n = 5). For the control panel, the data are plotted as described in the legend for Fig. 4; the conditions used were the same as those described for the controls in Table I (n = 10).

resulted in their release into solution. In only one case was some digoxigenin-labeled product found in a recovered PCR reaction mixture; in this instance, the sections had been subjected to PCR without prior DNase treatment or RT, and the PCR had been carried through 30 cycles with the COIII primers. Thus, the latter were able to target the multiple copies of the mitochondrial genome, apparently producing more product than could be retained in the section.

DISCUSSION

Organization of Pathway-Related Enzymes

In mammalian liver, the pathway of urea synthesis consists of five reactions, which occur in two separate cell compartments. The first two reactions take place in the mitochondrial matrix [Gamble and Lehninger, 1973; Clarke, 1976], and the next three in the cytoplasmic space [Ratner, 1976]. All the enzymes of the urea cycle are soluble proteins, meaning that they are found in the aqueous phase when cells or organelles are disrupted in the absence of detergent. Using isotope dilution techniques in incubations of intact and permeabilized liver mitochondria and hepatocytes, previous studies from this laboratory have shown that these five enzymes function in situ as if they are highly organized [Cohen et al., 1982, 1987, 1992; Cheung et al., 1989]; pathway intermediates are channeled between consecutive members of the pathway, even

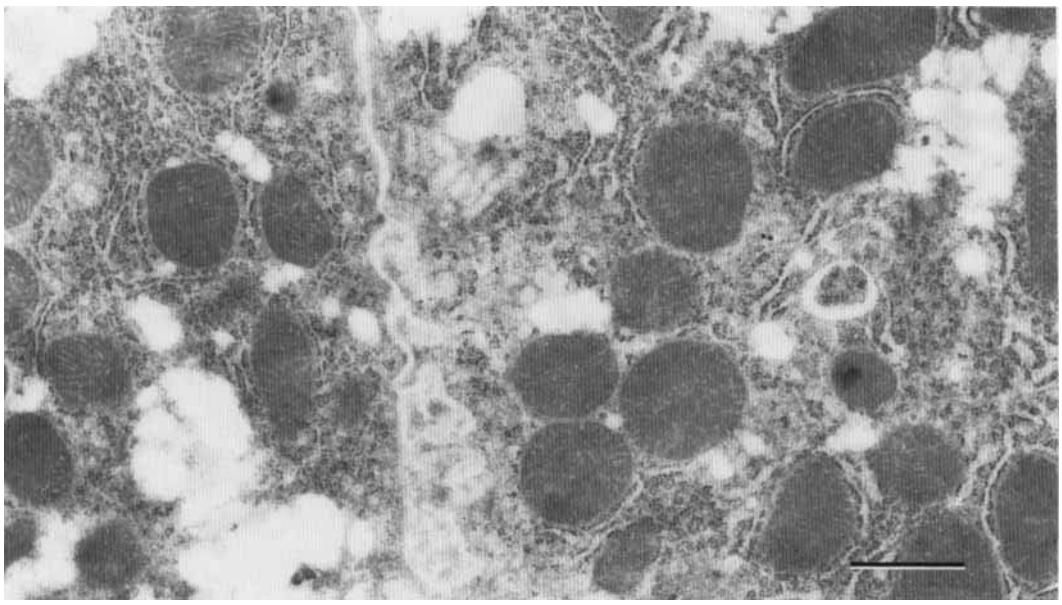

Fig. 7. Untreated section. The section shown was not subjected to any of the experimental procedures; it was stained with 3.5% uranyl acetate. Bar = 1 μm.

across the mitochondrial membranes [Cohen et al., 1987; Cheung et al., 1989]. The three cytoplasmic enzymes of the pathway, ASS, ASL, and arginase, were shown to be organized around the mitochondria by consideration of the combined facts that citrulline is channeled from ornithine transcarbamylase in the mitochondrial matrix to ASS in the cytoplasmic space and that subsequent intermediates are tightly channeled between ASS and ASL and between ASL and arginase [Cheung et al., 1989]. Immunocytochemical studies at the ultrastructural level confirmed that virtually all the ASS and ASL is located just outside the mitochondria in intact liver [Cohen and Kuda, 1996]. Some immunospecific protein is also found in the ER in the immediate vicinity of the mitochondria.

Stable channeling of intermediates between the urea cycle enzymes requires relatively stable protein–protein interactions, which may exist only under the unique conditions obtained in situ [Srere, 1987]. The molecular mechanisms leading to these interactions have not been identified; they may require the participation of other proteins of either the mitochondrial membranes or, for the cytoplasmic members of the cycle, of the ER or the cytoskeleton. Some of both of the latter structures are known to be associated with mitochondria [Shore and Tata, 1975; Summerhayes et al., 1983].

Since ASS and ASL are soluble enzymes, which do not retain their association with mitochondria when the latter are isolated, the present studies were designed to determine how the previously demonstrated intracellular localization of these proteins might be accomplished. Conceivably, this could involve targeting of either the proteins themselves, or their mRNAs. The results described here clearly show that targeting occurs at the mRNA level; ASS and ASL mRNAs are localized next to the mitochondria and in the adjacent ER in intact liver. In fact, because of the loss of ultrastructural detail in the treated sections, it is not possible to state with certainty that those mRNAs, which appear to be in the ER, are actually on the ER membranes. It is known that there are polyribosomes and rough ER closely associated with mitochondria in liver homogenates [Shore and Tata, 1975]. In the present work, many polyribosomes can be seen around the mitochondria in micrographs of untreated sections (Fig. 7). Studies in yeast, however, have demonstrated that mitochondrial-bound polyribosomes predominantly synthesize mitochondrial proteins [Ades and Butow, 1980; Suissa and Schatz, 1982]. Cytoplasmic proteins appear to be synthesized on free polyribosomes, not on the rough ER [Suissa and Schatz, 1982]. In fact, it is not known on which population of polyribosomes ASL and ASS mRNAs are translated. The results presented here, however, show that the particular polyribo-

somes involved are localized to the immediate vicinity of the mitochondrial outer membrane.

Targeting of the mRNAs to this site may be the first step of the mechanisms which result in the intracellular organization of ASL and ASS proteins. It has been pointed out [Bassell et al., 1994] that the targeting of particular mRNAs to limited regions within the cell would be a means of achieving high concentrations of newly synthesized proteins and favoring specific protein-protein interactions. We have now demonstrated several aspects of the organization of the pathway of urea synthesis in situ: the functional effects, i.e., channeling of intermediates; a mechanistic basis, namely the location of ASS and ASL; and a mechanism for the localization of these proteins, i.e., the sorting of the mRNAs.

The phenomenon of mRNA sorting has been described for proteins of the cytoskeleton [Sundell and Singer, 1990; Taneja et al., 1992; Fulton, 1993] and of developing myofibrils [Isaacs and Fulton, 1987; Morris and Fulton, 1994] and neurons [Kleiman et al., 1994], and for numerous proteins in nonmammalian oocytes (e.g., Pondel and King, 1988; Gottlieb, 1992; Mowry and Melton, 1992]. The targeting signal for virtually all of these mRNAs resides in the 3′-untranslated region [Gottlieb, 1992; Kislauskis et al., 1993, 1994; Hill and Gunning, 1993]. It has also been shown in cultured cells that misdirection of the mRNA of β-actin can result in an altered phenotype [Kislauskis et al., 1994]. The demonstration of mRNA sorting in somatic cells has been largely confined to structural elements, whose spatial orientations are relatively easily visualized; it has not previously been extended to the soluble proteins of metabolic pathways. Yet the organization of functionally related soluble enzymes into complex metabolic pathways presents demanding and precise requirements for the localization of specific enzyme proteins. The data presented here show that the targeting of the mRNAs of two such enzymes occurs in intact liver. Similar mRNA targeting may occur for other soluble cytoplasmic proteins that are known to function at or near the mitochondrial membrane, such as hexokinase [Wilson, 1980].

The organization of metabolically linked soluble enzymes into functional complexes in situ, as demonstrated for the urea cycle, may be an important and common characteristic of cells and organelles [Srere, 1987]. The unique conditions of very high protein concentration, molecular crowding, and extensive membrane systems and ultrastructural networks which exist within the cell have been reviewed in detail [Clegg, 1984; Srere, 1987]. All the evidence points to a cytoplasmic compartment in which many soluble macromolecules are excluded from much of the space and physically restricted to certain limited areas [Luby-Phelps, 1993]. All these factors favor intermolecular interactions [Minton, 1983]. If particular proteins can be delivered and segregated into restricted intracellular sites, and thus accumulate in locally high concentrations, specific protein–protein interactions could be more readily achieved. One way to accomplish this would be by targeting certain mRNAs to those particular sites for translation [Bassell et al., 1994]. Such a mechanism provides the possibility of additional levels of metabolic regulation, such as post-transcriptional alterations in the 3′-untranslated region targeting signals, or changes in the amounts of the RNA binding proteins responsible for transporting mRNAs to the appropriate location. The targeting of particular mRNAs to limited intracellular locations implies that there must also exist families of proteins which constitute the targets [Wilhelm and Vale, 1993]; the levels of these could also vary under different metabolic conditions.

There are complex interactions between the cytoskeleton and components of the apparatus of protein synthesis. Most poly(A)$^+$ RNA is associated with the cytoskeleton, primarily with the actin filaments or the microtubules [Taneja et al., 1992; Bassell et al., 1994]; these structural elements appear to be involved in the transport and anchoring of the mRNA [Sundell and Singer, 1990; Taneja et al., 1992; Hamill et al., 1994]. Most polysomes are also associated with cytoskeletal elements [Lenk et al., 1977; Zambetti et al., 1990; Hesketh and Pryme, 1991; Taneja et al., 1992; Hamill et al., 1994]. It has been shown that the eukaryotic elongation factor EF1-α binds to actin filaments and microtubules; it crosslinks the former, and affects the polymerization state of the latter [reviewed by Condeelis, 1995]. The cytoskeleton, particularly the microtubules, also appears to be important in anchoring cellular organelles, and perhaps in controlling their intracellular movements [Summerhayes et al., 1983]. Each of the above associations is a potential site of regulation of the complex process of translation.

Methodology

To investigate the possible localization of ASL and ASS mRNAs it was necessary to be able to detect these species at the ultrastructural level. For this purpose, a method was developed to perform high-resolution in situ RT-PCR. In situ RT-PCR at the light microscope level has been described by other investigators [Nuovo et al., 1993], but the level of resolution is not sufficient to determine the precise intracellular location of specific mRNAs. At the time the present experiments were done, in situ RT-PCR at the electron microscope level had not been reported. Since then, the ultrastructural distribution of poly(A)$^+$ RNA in detergent-extracted cells has been determined by in situ RT [Bassell et al., 1994]. In the present studies, the method developed for in situ RT on thin sections was also successful in demonstrating the localization of ASL and ASS mRNAs; exactly the same results were obtained using in situ RT and in situ RT-PCR. The latter procedure was more powerful, however, producing more and larger silver grains.

In situ hybridization provides an alternative method for detection of specific mRNAs, and has been successfully accomplished at the electron microscope level [Pomeroy et al., 1991; Fischer et al., 1992; Bassell et al., 1994]. High-resolution in situ RT-PCR promises to be a more direct, simpler assay than in situ hybridization, with the potential for generating a more heavily labeled signal. This is a consideration of special importance for the visualization of individual mRNA species, in particular of species such as ASL and ASS mRNAs, which might be present in low amounts. In situ RT-PCR at the ultrastructural level, which has not previously been used to demonstrate the location of specific mRNAs, should prove to be a valuable technique for this purpose.

ACKNOWLEDGMENTS

This work was supported by grant GM44638 from the National Institutes of Health. The author thanks Ms. Aileen Kuda for the tissue preparation and for the electron microscopy of these difficult samples. The oligonucleotide primers were synthesized by the Microchemical Core Laboratory of the Norris Comprehensive Cancer Center at the University of Southern California. Part of this work was presented previously as an abstract and poster at the joint meeting of ASBMB/DBC-ACS, 1995 (Cohen, N.S., L.B. #33).

REFERENCES

Ades IZ, Butow RA (1980): The products of mitochondria-bound cytoplasmic polysomes in yeast. J Biol Chem 255: 9918–9924.

Amaya Y, Matsubasa T, Takiguchi M, Kobayashi K, Saheki T, Kawamoto S, Mori M (1988): Amino acid sequence of rat argininosuccinate lyase deduced from cDNA. J Biochem 103:177–181.

Attardi G, Schatz G (1988): Biogenesis of mitochondria. Annu Rev Cell Biol 4:289–333.

Bassell GJ, Powers CM, Taneja KL, Singer RH (1994): Single mRNAs visualized by ultrastructural in situ hybridization are principally localized at actin filament intersections in fibroblasts. J Cell Biol 126:863–876.

Cheung C-W, Cohen NS, Raijman L (1989): Channeling of urea cycle intermediates in situ in permeabilized hepatocytes. J Biol Chem 264:4038–4044.

Chomczynski P, Sacchi N (1987): Single-step method of RNA isolation by acid guanidinium thiocyanate-phenol-chloroform extraction. Anal Biochem 162:156–159.

Clarke S (1976): A major polypeptide component of rat liver mitochondria. J Biol Chem 251:950–961.

Clegg JS (1984): Properties and metabolism of the aqueous cytoplasm and its boundaries. Am J Physiol 246:R133–R151.

Cohen NS, Cheung C-W, Raijman L (1980): The effects of ornithine on mitochondrial carbamyl phosphate synthesis. J Biol Chem 255:10248–10255.

Cohen NS, Cheung C-W, Kyan FS, Jones EE, Raijman L (1982): Mitochondrial carbamyl phosphate and citrulline synthesis at high matrix acetylglutamate. J Biol Chem 257:6898–6907.

Cohen NS, Kuda A (1996): Localization of argininosuccinate synthetase and argininosuccinate lyase around mitochondria by immunocytochemistry. J Cell Biochem (in press).

Cohen NS, Kyan FS, Kyan SS, Cheung C-W, Raijman L (1985): The apparent K_m of ammonia for carbamoyl phosphate synthetase (ammonia) in situ. Biochem J 229:205–211.

Cohen NS, Cheung C-W, Raijman L (1987): Channeling of extramitochondrial ornithine to matrix ornithine transcarbamylase. J Biol Chem 262:203–208.

Cohen NS, Cheung C-W, Sijuwade E, Raijman L (1992): Kinetic properties of carbamoyl–phosphate synthase (ammonia) and ornithine carbamoyltransferase in permeabilized mitochondria. Biochem J 282:173–180.

Condeelis J (1995): Elongation factor 1α, translation and the cytoskeleton. Trends Biochem Sci 20:169–170.

Fischer D, Weisenberger D, Scheer U (1992): In situ hybridization of digoxigenin-labeled rRNA probes to mouse liver ultrathin sections. In Boehringer Mannheim "Nonradioactive In Situ Hybridization Application Manual." Boehringer Mannheim GmbH-Biochemica, Mannheim, Germany pp 56–58.

Fulton AB (1993): Spatial organization of the synthesis of cytoskeletal proteins. J Cell Biochem 52:148–152.

Gadeleta G, Pepe G, DeCandia G, Quagliariello C, Sbisa E, Saccone C (1989): The complete nucleotide sequence of the *Rattus norvegicus* mitochondrial genome: Cryptic signals revealed by comparative analysis between vertebrates. J Mol Evol 28:497–516.

Gamble JD, Lehninger AL (1973): Transport of ornithine and citrulline across the mitochondrial membrane. J Biol Chem 248:610–618.

Gottlieb E (1992): The 3′-untranslated region of localized maternal messages contains a conserved motif involved in mRNA localization. Proc Natl Acad Sci USA 89:7164–7168.

Hamill D, Davis J, Drawbridge J, Suprenant KA (1994): Polyribosome targeting to microtubules: Enrichment of specific mRNAs in a reconstituted microtubule preparation from sea urchin embryos. J Cell Biol 127:973–984.

Hesketh JE, Pryme IF (1991): Interaction between mRNA, ribosomes and the cytoskeleton. Biochem J 277:1–10.

Hill MA, Gunning P (1993): Beta and gamma actin mRNAs are differentially located within myoblasts. J Cell Biol 122:825–832.

Horikoshi T, Danenberg KD, Stadlbauer THW, Volkenandt M, Shea LCC, Aigner K, Gustavsson B, Leichman L, Frosing R, Ray M, Gibson NW, Spears CP, Danenberg PV (1992): Quantitation of thymidylate synthase, dihydrofolate reductase, and DT-diaphorase gene expression in human tumors using the polymerase chain reaction. Cancer Res 52:108–116.

Isaacs WB, Fulton AB (1987): Cotranslational assembly of myosin heavy chain in developing cultured skeletal muscle. Proc Natl Acad Sci USA 84:6174–6178.

Jones MD, Foulkes NS (1989): Reverse transcription of mRNA by *Thermus aquaticus* DNA polymerase. Nucleic Acids Res 17:8387–8388.

Kislauskis EH, Li Z, Singer RH, Taneja KL (1993): Isoform-specific 3′-untranslated sequences sort α-cardiac and β-cytoplasmic actin messenger RNAs to different cytoplasmic compartments. J Cell Biol 123:165–172.

Kislauskis EH, Zhu X, Singer RH (1994): Sequences responsible for intracellular localization of β-actin messenger RNA also affect cell phenotype. J Cell Biol 127:441–451.

Kleiman R, Banker G, Steward O (1994): Development of subcellular mRNA compartmentation in hippocampal neurons in culture. J Neurosci 14:1130–1140.

Lenk R, Ransom L, Kaufman Y, Penman S (1977): A cytoskeletal structure with associated polyribosomes obtained from HeLa cells. Cell 10:67–78.

Luby-Phelps K (1993): Effect of cytoarchitecture on the transport and localization of protein synthetic machinery. J Cell Biochem 52:140–147.

Minton AP (1983): The effect of volume occupancy upon the thermodynamic activity of proteins: Some biochemical consequences. Mol Cell Biochem 55:119–140.

Morris EJ, Fulton AB (1994): Rearrangement of mRNAs for costamere proteins during cultured skeletal muscle from chicken. J Cell Sci 107:377–386.

Morris SM Jr, Moncman CL, Rand KD, Dizikes GJ, Cederbaum SD, O'Brien WE (1987): Regulation of mRNA levels for five urea cycle enzymes in rat liver by diet, cyclic AMP, and glucocorticoids. Arch Biochem Biophys 256:343–353.

Mowry KL, Melton DA (1992): Vegetal messenger RNA localization directed by a 340-nt RNA sequence element in *Xenopus* oocytes. Science 255:991–994.

Nuovo GJ, Lidonnici K, MacConnell P, Lane B (1993): Intracellular localization of polymerase chain reaction (PCR)-amplified hepatitis C cDNA. Am J Surg Pathol 17:683–690.

Pomeroy ME, Lawrence JB, Singer RH, Billings-Gagliardi S (1991): Distribution of myosin heavy chain mRNA in embryonic muscle tissue visualized by ultrastructural in situ hybridization. Dev Biol 143:58–67.

Pondel MD, King ML (1988): Localized maternal mRNA related to transforming growth factor β mRNA is concentrated in a cytokeratin-enriched fraction from *Xenopus* oocytes. Proc Natl Acad Sci USA 85:7612–7616.

Ratner S (1976): The enzymes of arginine and urea synthesis. Adv Enzymol 39:1–90.

Shaffer AL, Wojnar W, Nelson W (1990): Amplification, detection, and automated sequencing of gibbon interleukin-2 mRNA by *Thermus aquaticus* DNA polymerase reverse transcription and polymerase chain reaction. Anal Biochem 190:292–296.

Shore GC, Tata JR (1975): Two fractions of rough endoplasmic reticulum from rat liver. I. Recovery of rapidly sedimenting endoplasmic reticulum in association with mitochondria. J Cell Biol 72:714–725.

Srere PA (1982): The structure of the mitochondrial inner membrane–matrix compartment. Trends Biochem Sci 7:375–378.

Srere PA (1987): Complexes of sequential metabolic enzymes. Annu Rev Biochem 56:89–124.

Suissa M, Schatz G (1982): Import of proteins into mitochondria. Translatable mRNAs for imported mitochondrial proteins are present in free as well as mitochondria-bound cytoplasmic polysomes. J Biol Chem 257:13048–13055.

Summerhayes IC, Wong D, Chen LB (1983): Effect of microtubules and intermediate filaments on mitochondrial distribution. J Cell Sci 61:87–105.

Sundell CL, Singer RH (1990): Actin mRNA localizes in the absence of protein synthesis. J Cell Biol 111:2397–2403.

Surh LC, Morris SM, O'Brien WE, Beaudet AL (1988): Nucleotide sequence of the cDNA encoding the rat argininosuccinate synthetase. Nucleic Acids Res 16:9352.

Taneja KL, Lifshitz LM, Fay FS, Singer RH (1992): Poly(A) RNA codistribution with microfilaments: Evaluation by in situ hybridization and quantitative digital imaging microscopy. J Cell Biol 119:1245–1260.

Weibel ER, Bolender RP (1973): Stereological techniques for electron microscopic morphometry. In Hayat MA (ed): "Principles and Techniques of Electron Microscopy: Biological Applications." New York: Van Nostrand-Reinhold, vol. 3, pp 239–312.

Wilhelm JE, Vale RD (1993): RNA on the move: the mRNA localization pathway. J Cell Biol 123:269–274.

Wilson JE (1980): Brain hexokinase, the prototype ambiquitous enzyme. Curr Topics Cell Regul 16:1–54.

Zambetti G, Wilming L, Fey EG, Penman S, Stein J, Stein G (1990): Differential association of membrane-bound and non-membrane-bound polysomes with the cytoskeleton. Exp Cell Res 191:246–255.